

Article

Adaptive Phasor Estimation Algorithm Based on a Least Squares Method

Woo-Joong Kim, Soon-Ryul Nam and Sang-Hee Kang * 

Department of Electrical Engineering, Myongji University, Yongin 17058, Korea; goodaltair@gmail.com (W.-J.K.); ptsouth@mju.ac.kr (S.-R.N.)

* Correspondence: shkang@mju.ac.kr; Tel.: +82-31-330-6364

Received: 11 March 2019; Accepted: 7 April 2019; Published: 10 April 2019



Abstract: This paper proposes an adaptive phasor estimation algorithm based on a least square method that can suppress the adverse effect of an exponentially decreasing DC offset component in a phasor estimation process. The proposed algorithm is composed of three stages: a basic least squares model, a time constant calculation, and an adaptive least squares model. First, we use the basic least squares model to estimate the parameter of the DC offset component in the fault current signal. This model is designed to incorporate fundamental frequency, and harmonic and constant components. Second, we use the estimated parameter to calculate the time constant of the DC offset component. Third, we redesign a least squares model that incorporates fundamental frequency, harmonic components, and exponential function of the DC offset component. Since this model incorporates the exponential function of the DC offset component contained in the fault current signal, it estimates the phasor of the correct fundamental frequency component without influence of the DC offset component. We evaluated the performance of the proposed algorithm using computer generated signals and EMTP simulation signals. The evaluation results show that the proposed algorithm can effectively suppress the adverse influence of the exponentially decaying DC offset component.

Keywords: least squares method; phasor estimation; DC offset

1. Introduction

Accurate phasor estimation of current and voltage signals is very important for the protection and control of a power system. When a power system fault occurs, the current signal may include noise components such as an exponentially decaying DC offset and high-frequency due to traveling waves in addition to the fundamental frequency component. This noise degrades phasor estimation performance. The high-frequency components generated by a traveling wave may be both harmonic and non-harmonic. The most commonly used discrete Fourier transform (DFT) and least squares method (LSM) for phasor estimation can eliminate harmonic components. However, non-harmonic components are not completely removed using these phasor estimation methods and must be removed because they can cause errors in the phasor estimation result. The frequency band of the high-frequency components generated by a traveling wave is determined by the length of a power system's transmission line [1]. Therefore, the cut-off frequency of the low-pass filter used for a power system's protection relay should be chosen to be lower than the lowest frequency of high-frequency components generated by the traveling wave, thus suppressing the phasor estimation error caused by non-harmonic components generated by the traveling wave.

The exponentially decaying DC offset component contained in the fault current signal is not removed during the phasor estimation process and the filtering process by the low-pass filter, since the DC offset component is a non-periodic signal and its frequency spectrum includes all frequencies.

Therefore, the DC offset component should be carefully taken into consideration in calculating the phasor of the fundamental frequency component.

Many techniques have been proposed for estimating the phasor of the correct fundamental frequency component without the adverse effect of the exponentially decaying DC offset component of the fault current signal. These can be classified into three main groups.

In the first group, the exponentially decaying DC offset component contained in the fault current signal is first filtered out and the phasor of the fundamental frequency component is estimated from the filtered signal using a DFT. In [2], a digital mimic filter is proposed to suppress the DC offset component in a fault current signal. The digital mimic filter can completely remove the DC offset component only when the actual time constant of the fault current signal's DC offset component is the same as the mimic filter's time constant. In [3], a Kalman filter is proposed to eliminate the DC offset component, only when the time constant of the DC offset component is the same as that modeled in a state transition matrix. In [4], an algorithm that uses the average value of the fault current signal for one cycle is proposed. In [5,6], algorithms that use the integral value of the fault current signal during one cycle are proposed. These algorithms [4–6] cannot completely eliminate the DC offset component if its time constant is small.

The second group uses a DFT to estimate the phasor of the fundamental frequency component and then calculate and remove the error due to the DC offset component in the DFT's estimated phasor value. In [7–11], the error due to the DC offset component in the DFT's estimated phasor value is calculated and eliminated by using three successive estimated phasor values. However, these methods take one cycle plus two additional samples to estimate the correct phasor and are susceptible to high frequency noise. In [12], the error due to the DC offset component in the DFT's estimated phasor value is calculated and eliminated using the output of another DFT filter tuned at the n -th harmonic component. However, the performance of this algorithm is highly affected by random noise. In [13], a partial summation algorithm is proposed to eliminate the error due to the DC offset component in the DFT's estimated phasor value. However, if the DC offset component has a small time constant, this algorithm cannot completely eliminate the error due to the DC offset component in the DFT's estimated phasor value. In [14–16], the error due to the DC offset component in the DFT's estimated phasor value is calculated and eliminated using the outputs of the even- and odd-sample-set DFTs. In [17], the samples used for the DFT computation are split into four groups. The DFT then obtains an estimated phasor value from each of the four groups. Then, the parameters of the DC offset component are obtained from the four phasor results. In [18], the error due to the DC offset component in the DFT's estimated phasor value is calculated and eliminated by combining the DFT outputs from even and odd sample-sets obtained for a one cycle data window decimated by two and by four. In [19,20], algorithms using an average value over one cycle are proposed to estimate the error due to the DC offset component in the DFT's estimated phasor value. However, these methods [14–20] are disadvantageous because the high frequency noise components are amplified by the subtraction process that calculates the error due to the DC offset component.

The third group uses the least squares methods. These methods find a coefficient that minimizes the error between the input signal and the predefined signal. Therefore, the predefined signal must be selected appropriately. As in the techniques of the first two groups, it is necessary to consider both the harmonic components and the exponentially decaying DC offset component to achieve an accurate phasor estimate. In [21–26], the DC offset component is approximated to the first two or three terms of its Taylor series expansion. However, as in the first group of techniques, these methods cannot accurately approximate the DC offset component when the time constant of the DC offset component is small, so the estimated phasor of the fundamental frequency component will include the error due to the DC offset component.

In this paper, we propose an adaptive phasor estimation method based on a least squares method. This method estimates the time constant of the exponentially decaying DC offset component contained in a fault current signal and then redesigns the least squares model using the estimated time constant.

This approach estimates the phasor of the fundamental frequency component without the influence of the DC offset component. We tested the performance of the proposed algorithm by running it against computer-generated signals and EMTP simulation signals. To evaluate the algorithm’s performance, we compared the results produced by the proposed algorithm to the results obtained from the conventional DFT, the even/odd DFT [14], the modified DFT [10], and the conventional LSM [21].

2. Proposed Phasor Estimation Algorithm

2.1. Basic Least Squares Model

When a fault occurs in a power system, the current signal can be represented as the combination of a fundamental frequency component, a harmonic component, and an exponentially decaying DC offset component, as in:

$$y[k] = B_0 e^{-k\Delta t/\tau} + \sum_{n=1}^M B_n \cos\left(n \frac{2\pi}{N} k + \theta_n\right), \tag{1}$$

where, B_0 and τ are the magnitude and the time constant of an exponentially component, B_n and θ_n are the amplitude and the phase angle of the n -th harmonic component, Δt is the sampling interval, N is the number of samples per cycle, M is the maximum order of the harmonic components included in the current signal, and k is the sample index.

The harmonic components in Equation (1) can be expressed as follows using the trigonometric formula:

$$\begin{aligned} \sum_{n=1}^M B_n \cos\left(n \frac{2\pi}{N} k + \theta_n\right) &= B_1 \cos(\theta_1) \cdot \cos\left(\frac{2\pi}{N} k\right) - B_1 \sin(\theta_1) \cdot \sin\left(\frac{2\pi}{N} k\right) \\ &\dots + B_M \cos(\theta_M) \cdot \cos\left(M \frac{2\pi}{N} k\right) - B_M \sin(\theta_M) \cdot \sin\left(M \frac{2\pi}{N} k\right) \end{aligned} \tag{2}$$

The exponentially decaying DC offset component in Equation (1) can be expressed as the Taylor series expansion:

$$B_0 e^{-k\Delta t/\tau} = B_0 - B_0 \frac{k\Delta t}{\tau} + \frac{B_0}{2} \left(\frac{k\Delta t}{\tau}\right)^2 - \dots \tag{3}$$

The conventional least squares methods are designed using the first two or three terms of the Taylor series expansion of Equation (3) in order to consider the exponentially decaying DC offset component in the fault current signal. If the time constant of the DC offset component is small, this component cannot be approximated accurately.

In this paper’s proposed technique, we estimate the time constant of the DC offset component and then redesign the least squares model matrix to estimate an accurate phasor of the fundamental frequency component. In order to estimate this time constant, the basic least squares model is designed to incorporate fundamental frequency, harmonic and constant components as in:

$$\begin{bmatrix} y[k-N+1] \\ \vdots \\ y[k-2] \\ y[k-1] \\ y[k] \end{bmatrix} = \begin{bmatrix} \cos\left(\frac{2\pi}{N}\right) & -\sin\left(\frac{2\pi}{N}\right) & \dots & \cos\left(M\frac{2\pi}{N}\right) & -\sin\left(M\frac{2\pi}{N}\right) & 1 \\ \vdots & \vdots & \ddots & \vdots & \vdots & \vdots \\ \cos\left(\frac{2\pi}{N}(N-2)\right) & -\sin\left(\frac{2\pi}{N}(N-2)\right) & \dots & \cos\left(M\frac{2\pi}{N}(N-2)\right) & -\sin\left(M\frac{2\pi}{N}(N-2)\right) & 1 \\ \cos\left(\frac{2\pi}{N}(N-1)\right) & -\sin\left(\frac{2\pi}{N}(N-1)\right) & \dots & \cos\left(M\frac{2\pi}{N}(N-1)\right) & -\sin\left(M\frac{2\pi}{N}(N-1)\right) & 1 \\ \cos\left(\frac{2\pi}{N}(N)\right) & -\sin\left(\frac{2\pi}{N}(N)\right) & \dots & \cos\left(M\frac{2\pi}{N}(N)\right) & -\sin\left(M\frac{2\pi}{N}(N)\right) & 1 \end{bmatrix} \begin{bmatrix} B_1 \cos(\theta_1) \\ B_1 \sin(\theta_1) \\ \vdots \\ B_M \cos(\theta_M) \\ B_M \sin(\theta_M) \\ B_0(k) \end{bmatrix} \tag{4}$$

$$\begin{matrix} [Y] & [A_N] & [X_N] \\ N \times 1 & N \times (2M + 1) & (2M + 1) \times 1' \end{matrix}$$

where, Y is an N -by-1 vector of the input signals, A is an N -by- $(2M + 1)$ model matrix for the basic least squares method, and X is a $(2M + 1)$ -by-1 vector of coefficients.

Equation (4) can be briefly expressed as:

$$Y = A \cdot X \tag{5}$$

The unknown vector of coefficients in Equation (5) can be obtained as follows:

$$X = [A^T \cdot A]^{-1} \cdot A^T \cdot Y, \tag{6}$$

where, A^T is the transpose of the model matrix A .

If the model matrix for the basic least squares method is designed as shown in Equation (4) and the input signal is equal to Equation (1), the estimated vector of coefficients will include the influence of the exponentially decaying DC offset component. This is because the DC offset component is not considered in the model matrix.

2.2. Time Constant Calculation

The coefficient of the constant component ($B_0[k]$) among the coefficients estimated by the basic least squares model is expressed as:

$$B_0[k] = \frac{B_0}{N} \cdot \frac{(e^{-\frac{\Delta t}{\tau} \cdot (k-N+1)} - e^{-\frac{\Delta t}{\tau} \cdot k})}{(1 - e^{-\frac{\Delta t}{\tau}})} = \frac{B_0}{N} \cdot \frac{(1 - e^{-\frac{\Delta t}{\tau} \cdot N})}{(1 - e^{-\frac{\Delta t}{\tau}})} e^{\frac{\Delta t}{\tau} \cdot (k-N+1)} \tag{7}$$

As shown in Equation (7), the coefficient of the constant component is estimated as the mean value of the exponentially decaying DC offset component included in the data window of the basic least squares method. Appendix A contains proofs related to Equation (7).

The time constant (τ) of the exponentially decaying DC offset component is calculated as in Equation (8) using two successive coefficients of the constant component:

$$\frac{B_0[k]}{B_0[k-1]} = \frac{\frac{B_0}{N} \cdot (1 - e^{-\frac{\Delta t}{\tau} \cdot N}) / (1 - e^{-\frac{\Delta t}{\tau}}) \cdot e^{\frac{\Delta t}{\tau} \cdot (k-N+1)}}{\frac{B_0}{N} \cdot (1 - e^{-\frac{\Delta t}{\tau} \cdot N}) / (1 - e^{-\frac{\Delta t}{\tau}}) \cdot e^{\frac{\Delta t}{\tau} \cdot (k-N+2)}} = e^{-\Delta t / \tau} \tag{8}$$

Using Equation (8), the time constant of the exponentially decaying DC offset component can be obtained as:

$$\tau = \frac{-\Delta t}{\ln\left(\frac{B_0[k]}{B_0[k-1]}\right)} = \frac{-\Delta t}{\ln(e^{-\Delta t / \tau})} \tag{9}$$

2.3. Adaptive Least Squares Model

In order to estimate the exact coefficients without affecting the exponentially decaying DC offset component included in the current signal, the exponential function should be incorporated in the model matrix for the adaptive least squares method. Since the time constant of the DC offset component contained in the current signal is estimated in Equation (9), the adaptive least squares model can be designed as:

$$\begin{bmatrix} y[k-N+1] \\ \vdots \\ y[k-2] \\ y[k-1] \\ y[k] \end{bmatrix} = \begin{bmatrix} \cos(\frac{2\pi}{N}) & -\sin(\frac{2\pi}{N}) & \cdots & \cos(M\frac{2\pi}{N}) & -\sin(M\frac{2\pi}{N}) & e^{-\frac{\Delta t}{\tau}} \\ \vdots & \vdots & \ddots & \vdots & \vdots & \vdots \\ \cos(\frac{2\pi}{N}(N-2)) & -\sin(\frac{2\pi}{N}(N-2)) & \cdots & \cos(M\frac{2\pi}{N}(N-2)) & -\sin(M\frac{2\pi}{N}(N-2)) & e^{-\frac{\Delta t}{\tau}(N-2)} \\ \cos(\frac{2\pi}{N}(N-1)) & -\sin(\frac{2\pi}{N}(N-1)) & \cdots & \cos(M\frac{2\pi}{N}(N-1)) & -\sin(M\frac{2\pi}{N}(N-1)) & e^{-\frac{\Delta t}{\tau}(N-1)} \\ \cos(\frac{2\pi}{N}(N)) & -\sin(\frac{2\pi}{N}(N)) & \cdots & \cos(M\frac{2\pi}{N}(N)) & -\sin(M\frac{2\pi}{N}(N)) & e^{-\frac{\Delta t}{\tau}N} \end{bmatrix} \begin{bmatrix} B_1 \cos(\theta_1) \\ B_1 \sin(\theta_1) \\ \vdots \\ B_M \cos(\theta_M) \\ B_M \sin(\theta_M) \\ B_0(k) \end{bmatrix} \tag{10}$$

$\begin{bmatrix} Y \\ N \times 1 \end{bmatrix} \qquad \qquad \qquad \begin{bmatrix} A_N \\ N \times (2M + 1) \end{bmatrix} \qquad \qquad \qquad \begin{bmatrix} X_N \\ (2M + 1) \times 1' \end{bmatrix}$

where, Y is an N -by-1 vector of the input signals, A_N is an N -by- $(2M + 1)$ model matrix for new least squares method, and X_N is a $(2M + 1)$ -by-1 vector of new coefficients.

Equation (10) can be briefly expressed as:

$$Y = A_N \cdot X_N \quad (11)$$

The unknown vector of coefficients in Equation (11) can be obtained as:

$$X_N = [A_N^T \cdot A_N]^{-1} \cdot A_N^T \cdot Y \quad (12)$$

The newly designed least squares model takes the exponential terms in the model matrix into account so that the exponentially decaying DC offset component included in the input signal can be approximated accurately. Thus, the error due to the DC offset component is excluded from the phasor of the fundamental frequency component.

Figure 1 shows a flowchart of the proposed algorithm. A low-pass Butterworth filter prevents aliasing and removes non-harmonic components generated by traveling waves. The basic least squares model obtains the parameters of the exponentially decaying DC offset component contained in the fault current signal. The DC offset component's time constant is calculated from these parameters. An adaptive least squares model is designed taking into account the time constant of the exponentially decaying DC offset. Finally, the phasor of the fundamental frequency component is accurately estimated using the adaptive least squares model.

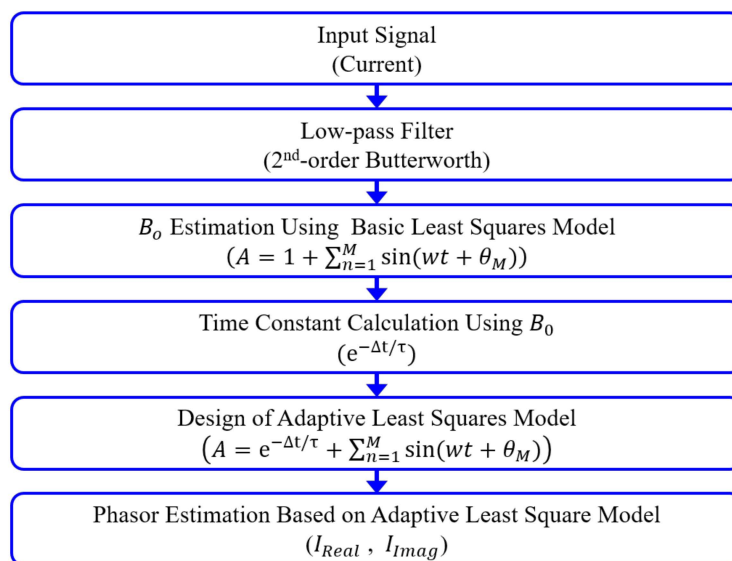


Figure 1. Flowchart of the Proposed Algorithm.

3. Case Studies

We evaluated the proposed algorithm's performance using computer-generated signals and EMTP-simulation signals. We compared these test results to those of the conventional DFT, the even/odd DFT [14], the modified DFT [10] and the conventional LSM [21].

To evaluate the accuracy of the proposed algorithm, we calculated the phasor estimation error to be:

$$\text{Error} = \frac{\text{reference RMS value} - \text{estimated RMS value}}{\text{reference RMS value}} \times 100\%, \quad (13)$$

where, the reference RMS value is the RMS value at 10 cycles after the fault.

In all cases, the sampling frequency was set to 7680 Hz (i.e., 128 sample per cycle in a 60 Hz System). The input signal was pre-processed by a second-order Butterworth low-pass filter with a gain

of 0.1 at a stop-band cut-off frequency of 750 Hz in order to remove high-frequency noises and prevent aliasing errors. Although the sampling frequency of the algorithm is 7680 Hz, the high-frequency noise that is higher than 750 Hz must be rejected by a preprocessing filter because the frequency band generated by a traveling wave in the assumed 100 km transmission line is 750~1500 Hz [1].

In the conventional least squares method, the model matrix is designed to include harmonic and exponentially decaying DC offset components. The harmonic components are included up to the 12th order and the exponentially decaying DC offset is derived from the first two terms of the Taylor series expansion in Equation (3). The data window length of the conventional least squares method is one cycle. In the proposed algorithm, the model matrix of the basic least square is designed to include the harmonic and constant components. The harmonic components are included up to the 12th order. The data window length of the proposed algorithm is one cycle.

3.1. Computer-Generated Signals

We evaluated the proposed algorithm's performance with computer-generated signals consisting of sinusoidal and exponentially decaying DC offset components. We investigated the algorithm's sensitivity to DC offset variation by running the tests with two different time constants ($0.5/f_0$ and $5/f_0$).

Case 1. Test for basic signals—the test signal was:

$$y[k] = 100e^{-k\Delta t/\tau} - 100\cos\left(\frac{2\pi}{N}k\right), \quad (14)$$

Figure 2 shows the test results for a time constant of $0.5/f_0$. As shown in Figure 2a, the result of the conventional DFT shows the largest transient overshoot and the largest oscillatory response. In Figure 2b, the proposed algorithm is seen to more accurately remove the adverse influence of the exponentially decaying DC offset than the other methods.

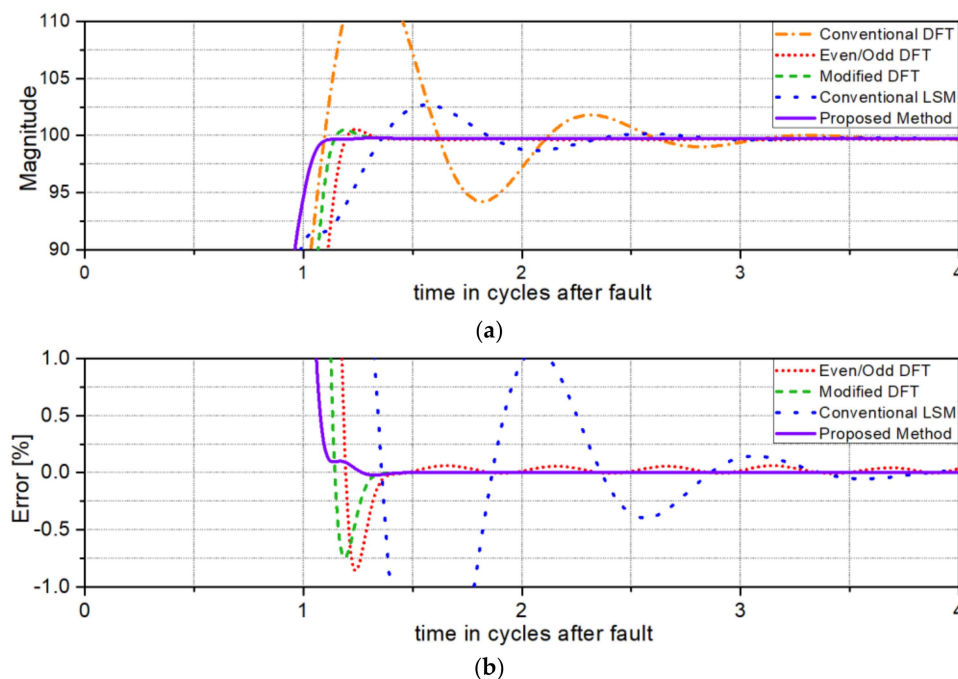


Figure 2. Test results for Case 1 ($\tau:0.5/f_0$): (a) Estimated RMS values; (b) errors.

Figure 3 shows the test results for a time constant of $5/f_0$. These results show the same performance advantage demonstrated in Figure 2 for a time constant of $0.5/f_0$.

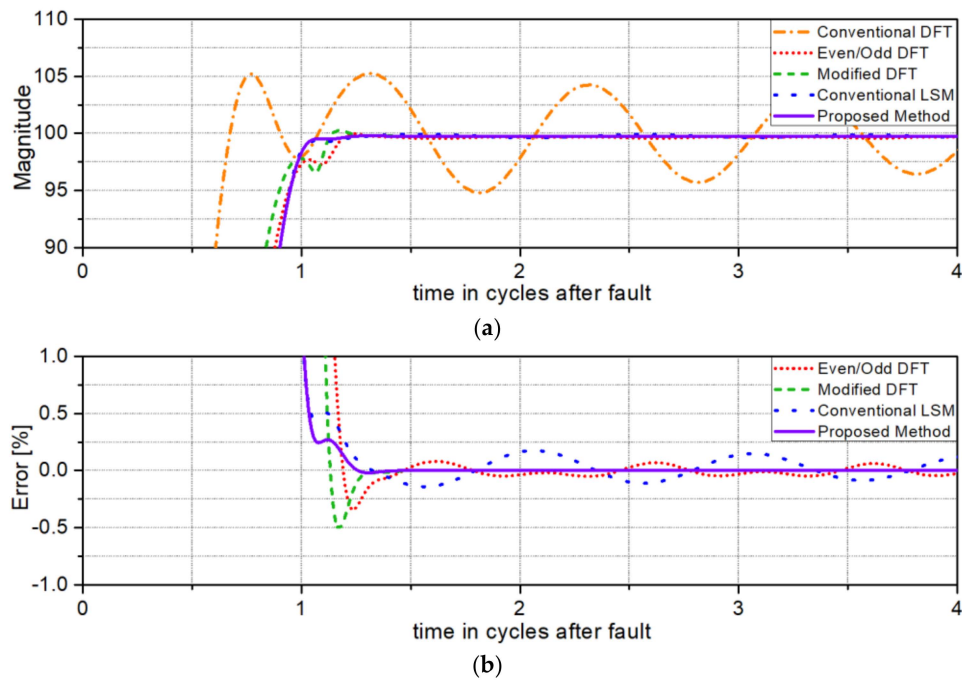


Figure 3. Test results for Case 1 ($\tau:5/f_0$): (a) Estimated RMS values; (b) errors.

Case 2. Test for Random Noise: In this case, the focus is on the noise immunity of the proposed algorithm. Gaussian white noise is added to the signal of Case 1. The signal-to-noise ratio (SNR) is set to 40 dB. The test signal used in this case is:

$$y[k] = 100e^{-k\Delta t/\tau} - 100\cos\left(\frac{2\pi}{N}k\right) + \text{Gaussian white noise} \quad (15)$$

Figures 4 and 5 show the robustness of the proposed algorithm in the presence of Gaussian white noise. Figure 4 shows the test results for a time constant of $0.5/f_0$.

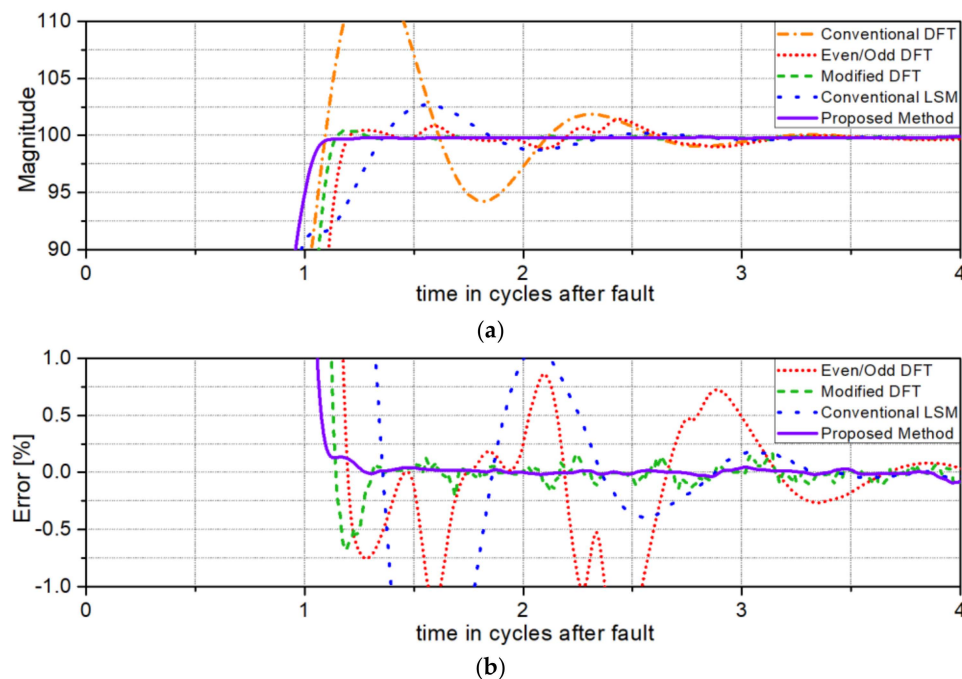


Figure 4. Test results for Case 2 ($\tau:0.5/f_0$): (a) Estimated RMS values; (b) errors.

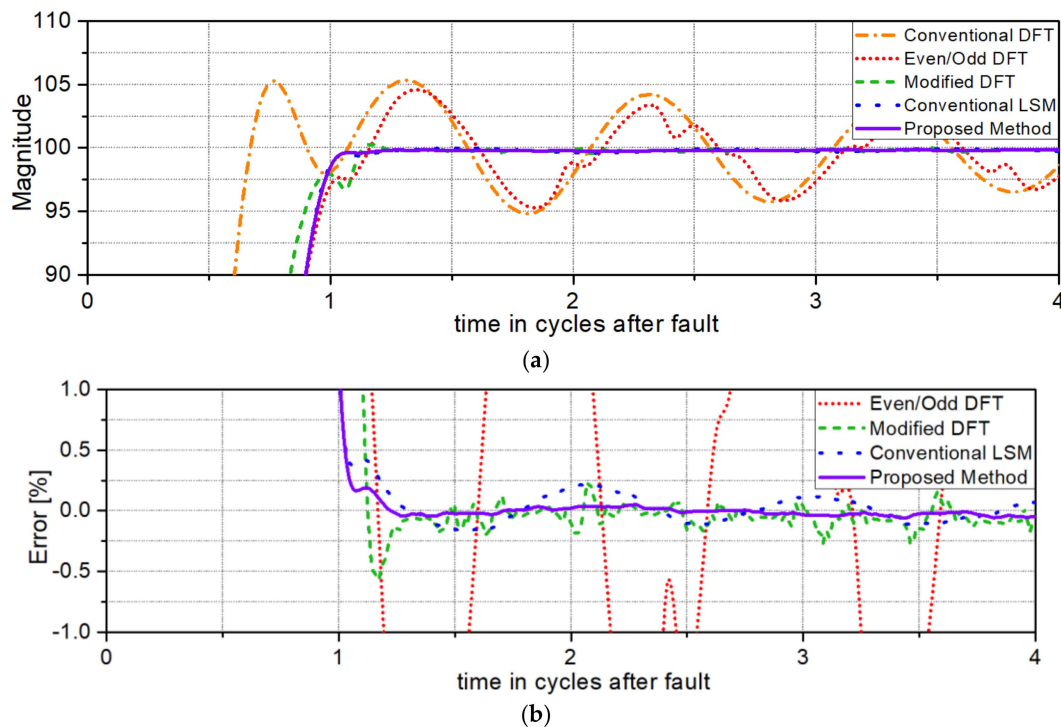


Figure 5. Test results for Case 2 ($\tau:5/f_0$): (a) Estimated RMS values; (b) errors.

As seen in Figure 4a, the result of the conventional DFT and the even/odd DFT show a very large transient overshoot and a very large oscillatory response. In Figure 4b, the proposed algorithm be seen to more accurately remove the adverse influence of the exponentially decaying DC offset than the other methods. Since the even/odd DFT and the modified DFT intrinsically use difference equations, an error occurs if a signal contains Gaussian white noise.

Figure 5 shows the test results for a time constant of $5/f_0$. As in the previous results for time constant $0.5/f_0$, the results for this time constant demonstrate that the proposed algorithm can more accurately remove the adverse influence of the exponentially decaying DC offset than the other methods.

The test results for the proposed algorithm show stable and superior results over the other methods, even when the signal contains Gaussian white noise.

3.2. EMTP Simulation Signals

The model system for the simulations is evaluated for a-g faults on a 154 kV, 100 km overhead transmission line with sources at both ends, as shown in Figure 6. The transmission line parameters used in the simulations are given in Table 1.

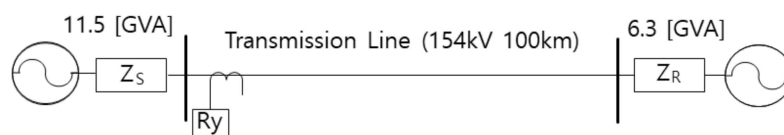


Figure 6. Single-line diagram of the model system.

The equivalent source parameters used in the simulation are given Table 2. The fault current signals are generated by the EMTP.

Table 1. Transmission line parameters.

Sequence	Parameter	Value	Units
Positive & Negative	R_1, R_2	0.0419	Ω/km
	L_1, L_2	0.8799	mH/km
	C_1, C_2	0.0128	$\mu\text{F}/\text{km}$
Zero	R_0	0.2294	Ω/km
	L_0	2.6666	mH/km
	C_0	0.0043	$\mu\text{F}/\text{km}$

Table 2. Equivalent source parameters.

Sequence	Source 1		Source 2	
	S [GVA]	X/R	R [GVA]	X/R
Positive & Negative	5.0	10.7	2.1	7.4
Zero	11.5	5.1	6.3	4.9

The magnitude and time constant of the exponentially decaying DC offset component varies depending on fault conditions such as fault location, fault resistance, and fault inception angle.

Figures 7–9 show the estimated RMS values and percent error of the fault current. The magnitude and time constant of the DC offset components depend on the fault distance from the relaying point to the fault point, so the performance of the proposed algorithm is evaluated by changing fault distance. A fault inception angle of 0° was used to maximize the magnitude of the DC offset component. Figure 7 shows the test results for a solid single-phase to ground fault at 10% of the total line length from the relaying point. As seen in Figure 7, the proposed algorithm accurately removes the adverse influence of the exponentially decaying DC offset more accurately than the conventional DFT, the even/odd DFT, and the conventional LSM, and also converges faster than the modified DFT.

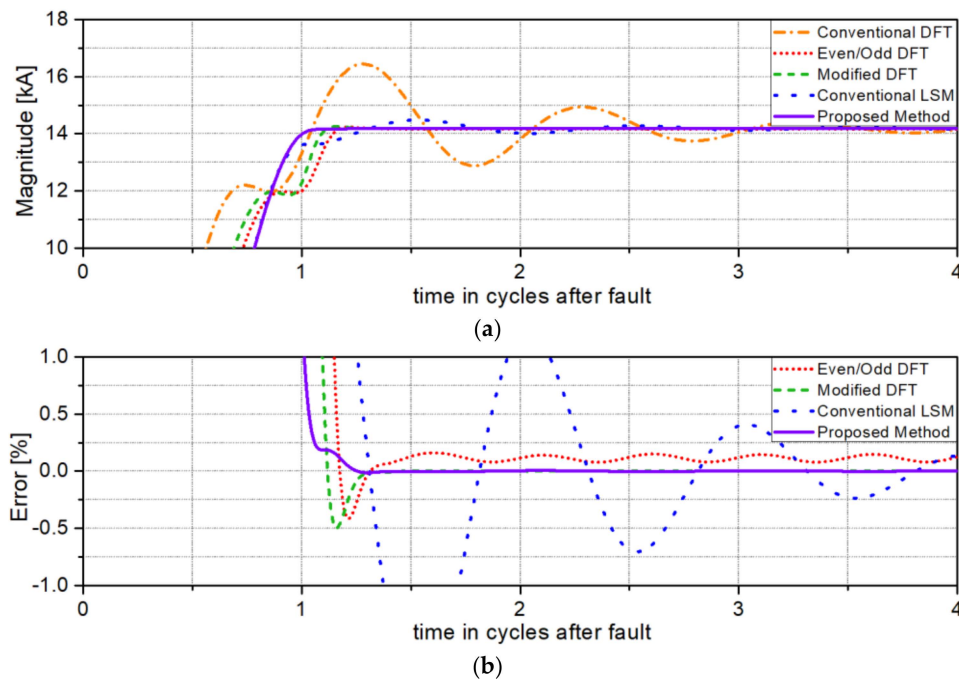


Figure 7. Test results for fault distance: 10%, fault inception angle: 0° : (a) Estimated RMS values; (b) errors.

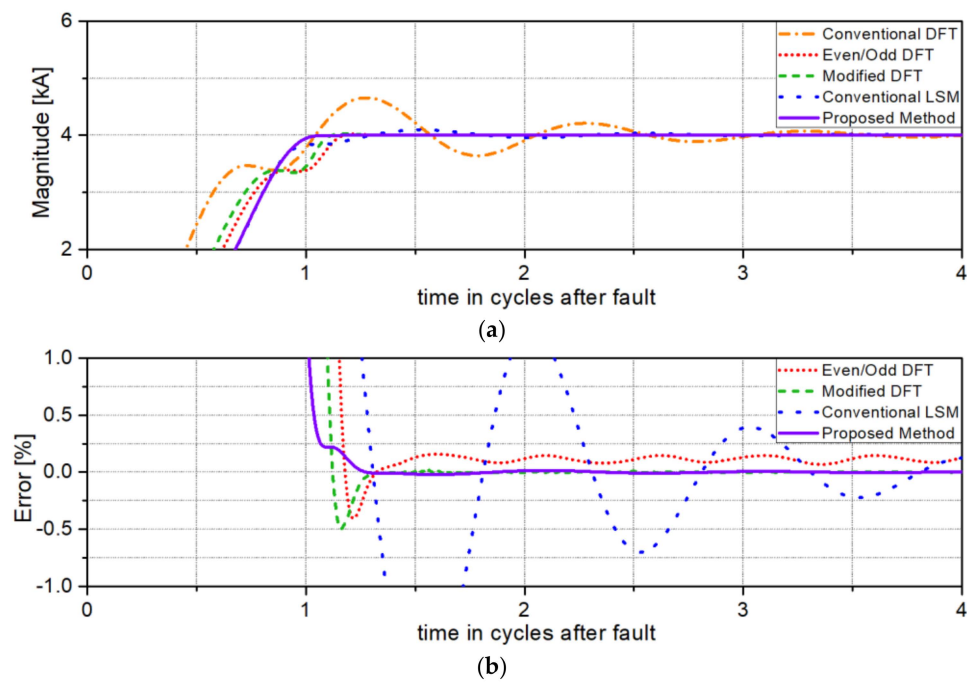


Figure 8. Test results for fault distance: 50%, fault inception angle: 0° : (a) Estimated RMS values; (b) errors.

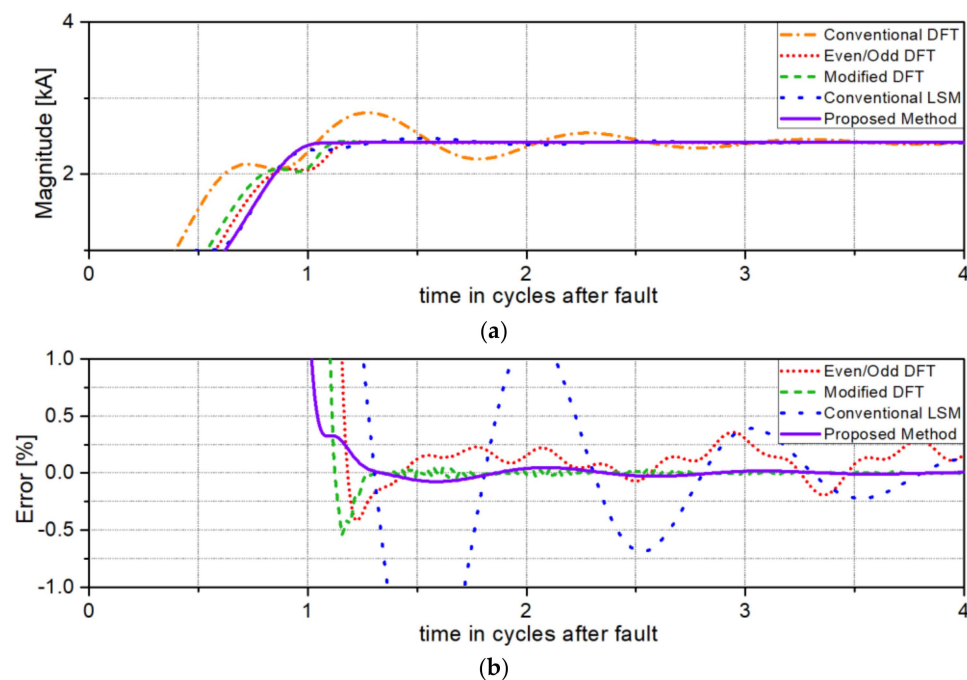


Figure 9. Test results for fault distance: 90%, fault inception angle: 0° . (a) Estimated RMS values; (b) errors.

Figure 8 shows the test results for solid single-phase to ground faults at 50% of the total line length from the relaying point. These results show the same performance advantage demonstrated in Figure 7 for the 10% distance.

Figure 9 shows the test results for solid single-phase to ground faults at 90% of the total line length from the relaying point. These results show the same performance advantages demonstrated in Figures 7 and 8 for their respective distances.

The magnitude and frequency band of the high-frequency components varies depending on fault conditions such as fault location, fault resistance, and fault inception angle.

Figures 10–12 show the estimated RMS values and percent error of the fault current. The magnitude and frequency band of the high-frequency components depend on the fault distance from the relaying point to the fault point; thus, as in the tests of Figures 7–9, the performance of the proposed algorithm is evaluated by changing fault distance. A fault inception angle of 90° was used to maximize the magnitude of the high-frequency component.

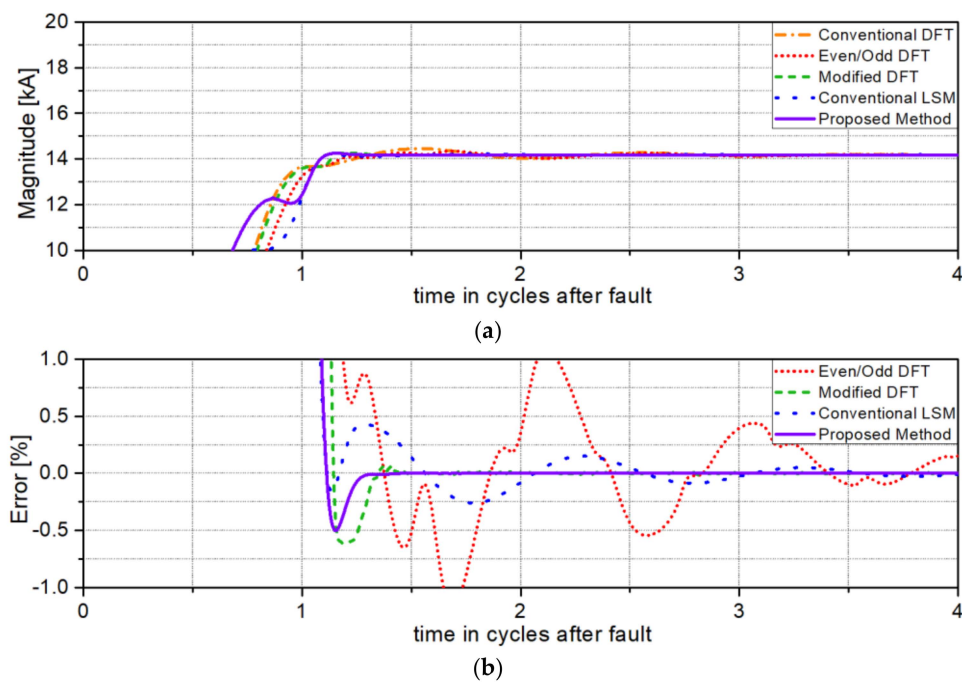


Figure 10. Test results for fault distance: 10%, fault inception angle: 90°: (a) Estimated RMS values; (b) errors.

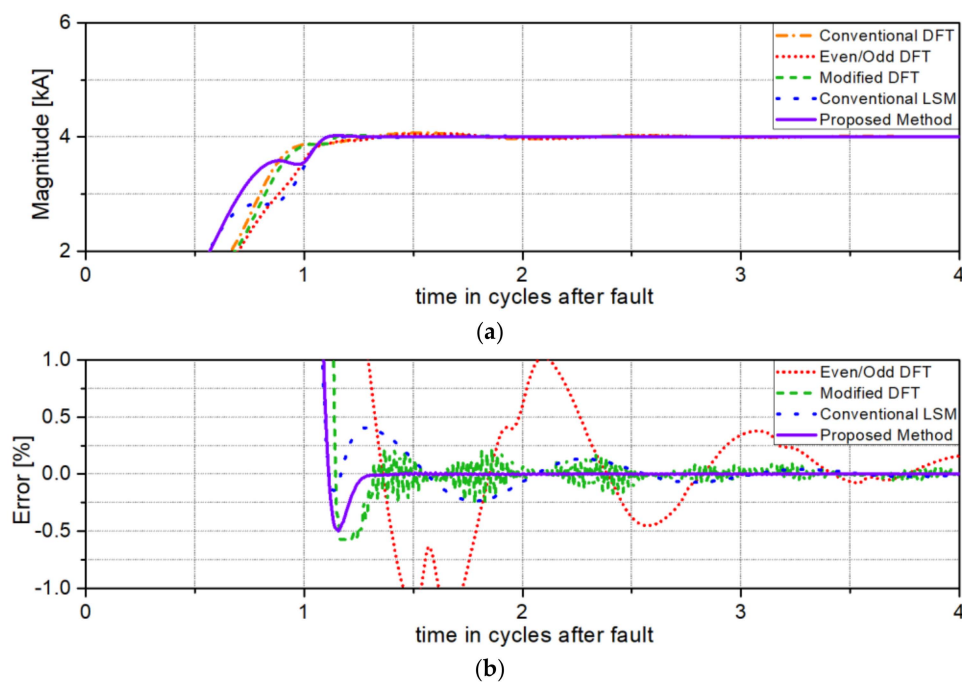


Figure 11. Test results for fault distance: 50%, fault inception angle: 90°. (a) Estimated RMS values; (b) errors.

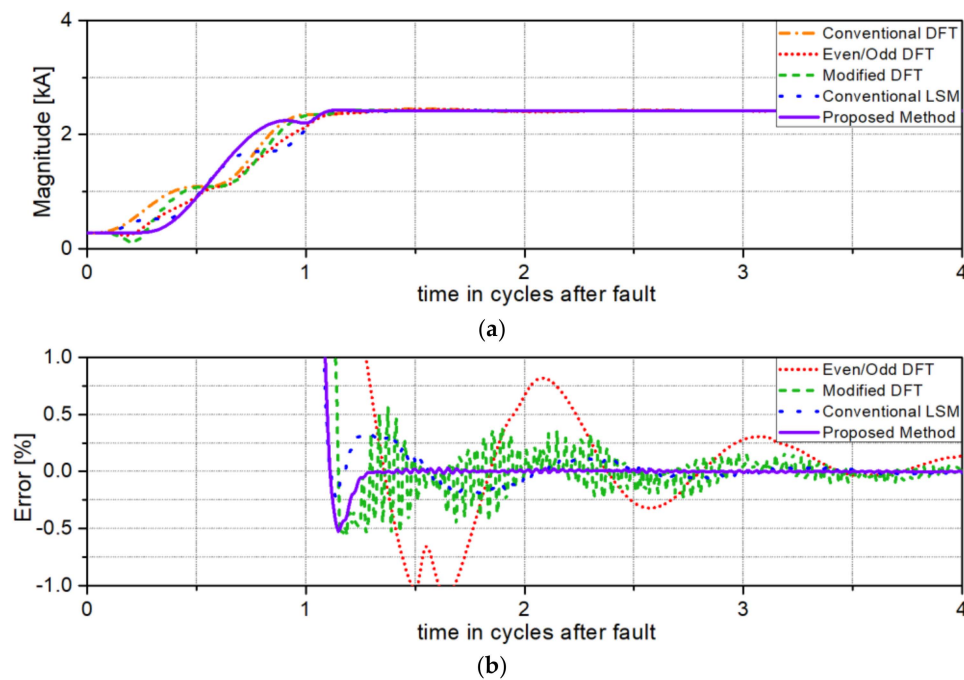


Figure 12. Test results for fault distance: 90%, fault inception angle: 90° . (a) Estimated RMS values; (b) errors.

Figure 10 shows the test results for a solid single-phase to ground fault at 10% of the total line length from the relaying point. As shown in Figure 10b, the proposed algorithm can more accurately estimate the phasor of the fundamental frequency component than the conventional DFT, the modified DFT, the even/odd DFT, and the conventional LSM.

Figure 11 shows the test results for a solid single-phase to ground fault at 50% of the total line length from the relaying point. These results show the same performance advantages demonstrated in Figure 10 for the 10% distance.

Figure 12 shows the test results for a solid single-phase to ground fault at 90% of the total line length from the relaying point. These results show the same performance advantages demonstrated in Figures 10 and 11 for their respective distances.

The EMTP test results show that, the proposed algorithm can both remove the exponentially decaying DC offset and accurately estimate the phasor of the fundamental frequency component when the signal contains high-frequency noise components.

4. Conclusions

In this paper, we proposed an adaptive phasor estimation algorithm based on a least squares method. The proposed algorithm estimates the time constant of the exponentially decaying DC offset component in the fault current signal first and redesigns the model matrix for the least squares model using the estimated time constant, and finally estimates the phasor of the fundamental frequency component using the redesigned least squares model. The result is that the phasor of the fundamental frequency component can be accurately estimated without the influence of the exponentially decaying DC offset component. The performance of the proposed algorithm was evaluated using computer-generated signals and EMTP simulation signals. Several computer-simulated signals, which take into account the fundamental frequency, exponentially decaying DC offset, and Gaussian white noise components, are used. The evaluation results show that the proposed algorithm can effectively suppress the adverse influence of the exponentially decaying DC offset and Gaussian white noise components and that the phasor of the fundamental frequency component can be accurately

and quickly estimated. Future research will be focused on research to reduce the computational complexity of the least squares method.

Author Contributions: Conceptualization, W.-J.K. and S.-H.K.; Methodology, W.-J.K. and S.-H.K.; Software, W.-J.K.; Validation, W.-J.K., S.-R.N. and S.-H.K.; Formal Analysis, W.-J.K. and S.-H.K.; Investigation, W.-J.K. and S.-R.N.; Writing-Original Draft Preparation, W.-J.K.; Writing-Review & Editing, W.-J.K., S.-R.N. and S.-H.K.

Funding: This research was supported by Korea Electric Power Corporation, Grant Number R17XA05-2 and R18XA01.

Conflicts of Interest: The authors declare no conflict of interest.

Appendix A

In the least squares method, the straight line ($y = b$) is fitted through the given points $(x_1, y_1), \dots, (x_n, y_n)$ so that the sum of the squares of the distances of those points from the straight line is at a minimum, where the distance is measured in the vertical direction (the y -direction) [27].

The point on the line with abscissa x_j has the b . Hence, its distance from (x_j, y_j) is $|y_j - b|$ in Figure A1 and that sum of squares is:

$$\varepsilon = \sum_{j=1}^n (y_j - b)^2$$

ε depends on b . A necessary condition for ε to be minimum is

$$\frac{\partial \varepsilon}{\partial b} = \frac{\partial}{\partial b} \sum_{j=1}^n (y_j - b)^2 = 2b \sum_{j=1}^n (1) - 2 \sum_{j=1}^n (y_j) = 0$$

The above equation can be expressed as:

$$b = \frac{\sum_{j=1}^n (y_j)}{\sum_{j=1}^n (1)}$$

If the input value y_j is an exponentially decaying DC offset component, the coefficient value b is as follows:

$$b = \frac{\sum_{j=1}^n B_0 \cdot e^{-\frac{\Delta t}{\tau} j}}{\sum_{j=1}^n 1} = \frac{B_0 (1 - e^{-\frac{\Delta t}{\tau} n})}{n (1 - e^{-\frac{\Delta t}{\tau}})}$$

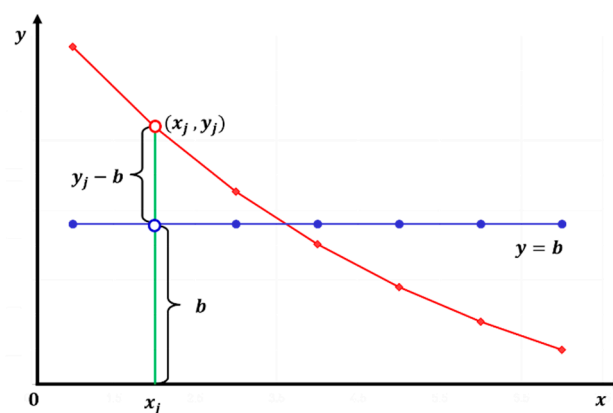


Figure A1. Vertical distance of a point (x_j, y_j) from a straight line $y = b$.

References

1. Swift, G.W. The spectra of fault-induced transients. *IEEE Trans. Power Appar. Syst.* **1979**, *98*, 940–947. [[CrossRef](#)]
2. Girgis, A.A. A new kalman filtering based digital distance relay. *IEEE Trans. Power Appar. Syst.* **1982**, *101*, 3471–3480. [[CrossRef](#)]
3. Benmouyal, G. Removal of DC-offset in current waveforms using digital mimic filtering. *IEEE Trans. Power Deliv.* **1995**, *10*, 621–630. [[CrossRef](#)]
4. Eisa, A.A.A.; Ramar, K. Removal of decaying DC offset in current signals for power system phasor estimation. In Proceedings of the 43rd International Universities Power Engineering Conference, Padova, Italy, 1–4 September 2008. [[CrossRef](#)]
5. Cho, Y.-S.; Lee, C.-K.; Jang, G.; Lee, H.J. An innovative decaying DC component estimation algorithm for digital relaying. *IEEE Trans. Power Deliv.* **2009**, *24*, 73–78. [[CrossRef](#)]
6. Abdoos, A.A.; Gholamian, S.A.; Farzinfar, M. Accurate and fast DC offset removal method for digital relaying schemes. *IET Gener. Transm. Distrib.* **2016**, *10*, 1769–1777. [[CrossRef](#)]
7. Gu, J.-C.; Yu, S.-L. Removal of DC offset in current and voltage signals using a novel fourier filter algorithm. *IEEE Trans. Power Deliv.* **2000**, *15*, 73–79. [[CrossRef](#)]
8. Yu, S.-L.; Gu, J.-C. Removal of decaying dc in current and voltage signals using a modified fourier filter algorithm. *IEEE Trans. Power Deliv.* **2001**, *16*, 372–379. [[CrossRef](#)]
9. Nam, S.-R.; Kang, S.-H.; Park, J.-K. An analytic method for measuring accurate fundamental frequency components. *IEEE Trans. Power Deliv.* **2002**, *17*, 405–411. [[CrossRef](#)]
10. Hwang, J.K.; Song, C.K.; Jeong, M.G. DFT-based phasor estimation for removal of the effect of multiple DC components. *IEEE Trans. Power Deliv.* **2018**, *33*, 2901–2909. [[CrossRef](#)]
11. Kim, W.-J.; Kagn, S.-H. A DC offset removal algorithm based on AR model. *J. Int. Counc. Electr. Eng.* **2018**, *8*, 156–162. [[CrossRef](#)]
12. Sidhu, T.S.; Zhang, X.; Albasri, F.; Sachdev, M.S. Discrete-fourier-transform-based technique for removal of decaying DC offset from phasor estimates. *IEE Proc. Gener. Transm. Distrib.* **2003**, *150*, 745–752. [[CrossRef](#)]
13. Guo, Y.; Kezunovic, M.; Chen, D. Simplified algorithms for removal of the effect of exponentially decaying DC-offset on the fourier algorithm. *IEEE Trans. Power Deliv.* **2003**, *18*, 711–717. [[CrossRef](#)]
14. Kang, S.-H.; Lee, D.-G.; Nam, S.-R.; Crossley, P.A.; Kang, Y.-C. Fourier transform-based modified phasor estimation method immune to the effect of the DC offsets. *IEEE Trans. Power Deliv.* **2009**, *24*, 1104–1111. [[CrossRef](#)]
15. Rahmati, A.; Adhami, R. An accurate filtering technique to mitigate transient decaying DC offset. *IEEE Trans. Power Deliv.* **2014**, *29*, 966–968. [[CrossRef](#)]
16. Silva, K.M.; Nascimento, F.A.O. Modified DFT-based phasor estimation algorithms for numerical relaying applications. *IEEE Trans. Power Deliv.* **2018**, *33*, 1165–1173. [[CrossRef](#)]
17. Yu, C.-S.; Huang, Y.-S.; Jiang, J.-A. A Full- and Half-Cycle DFT-based Technique for Fault Current Filtering. In Proceedings of the 2010 IEEE International Conference on Industrial Technology, Vina del Mar, Chile, 14–17 March 2010. [[CrossRef](#)]
18. Silva, K.M.; Kusel, B.F. DFT based phasor estimation algorithm for numerical digital relaying. *Electron. Lett.* **2013**, *49*, 412–414. [[CrossRef](#)]
19. Dadash, M.R.; Zhang, Z. A new DFT-based current phasor estimation for numerical protective relaying. *IEEE Trans. Power Deliv.* **2013**, *28*, 2172–2179. [[CrossRef](#)]
20. Jafarpisheh, B.; Madani, S.M.; Shahrtash, S.M. A new DFT-based estimation algorithm using high-frequency modulation. *IEEE Trans. Power Deliv.* **2017**, *32*, 2416–2423. [[CrossRef](#)]
21. Sachdev, M.S.; Baribeau, M.A. A new algorithm for digital impedance relays. *IEEE Trans. Power Apparatus Syst.* **1979**, *98*, 2232–2240. [[CrossRef](#)]
22. Rahman, M.A.; Dash, P.K.; Dowton, E.R. Digital protection of power transformer based on weighted least square algorithm. *IEEE Trans. Power Appar. Syst.* **1982**, *101*, 4204–4210. [[CrossRef](#)]
23. Isaksson, A. Digital protective relaying through recursive least-squares identification. *IEE Proc. C Gener. Transm. Distrib.* **1988**, *135*, 441–449. [[CrossRef](#)]
24. Sachdev, M.S.; Nagpal, M. A recursive least error squares algorithm for power system relaying and measurement applications. *IEEE Trans. Power Deliv.* **1991**, *6*, 1008–1015. [[CrossRef](#)]

25. Belega, D.; Petri, D. Dynamic synchrophasor estimation in the presence of decaying DC offsets. In Proceedings of the 2014 IEEE International Instrumentation and Measurement Technology Conference (I2MTC), Montevideo, Uruguay, 12–15 May 2014. [[CrossRef](#)]
26. Jafarian, P.; Sanaye-Pasand, M. Weighted least error squares based variable window phasor estimator for distance relaying application. *IET Gener. Transm. Distrib.* **2011**, *5*, 298–306. [[CrossRef](#)]
27. Kreyszig, E. *Advanced Engineering Mathematics*, 10th ed.; John Wiley & Sons, Inc.: Hoboken, NJ, USA, 2008; pp. 872–873, ISBN 978-0-470-45836-5.



© 2019 by the authors. Licensee MDPI, Basel, Switzerland. This article is an open access article distributed under the terms and conditions of the Creative Commons Attribution (CC BY) license (<http://creativecommons.org/licenses/by/4.0/>).